Ayad Abbood Abdulhasan<sup>1</sup>, Ali J. Naisan<sup>2</sup>,Kareem Mohsen Raheef<sup>3</sup>, Wael H. Alsadi<sup>4</sup>,F. F. Sayyid <sup>5</sup>, A. M. Mustafa <sup>5</sup>, A. Al-Amiery<sup>6</sup>, A. H. Kadhum<sup>7</sup>

<sup>1</sup>Department of Metallurgy Engineering, Al-Mustafa University, Baghdad, Iraq, <sup>2</sup>Ministry of Oil State Company for gas filling and services, Baghdad, Iraq, <sup>3</sup>Ashur university college, Baghdad, Iraq, <sup>4</sup>Department of Chemistry, Faculity of Science, Taibah University, Al-Madinah Al-Munawarah, Medina, Saudi Arabiam, <sup>5</sup>Production Engineering and Metallurgy, University of Technology, Baghdad, Iraq, <sup>6</sup>Al-Ayen Scientific Research Center, Al-Ayen Iraqi University, AUIQ, An Nasiriyah, Thi Qar, Iraq, <sup>7</sup>Faculty of Medicine, University of Al-Ameed, Karbala, Iraq

Scientific paper ISSN 0351-9465, E-ISSN 2466-2585 https://doi.org/10. 62638/ZasMat1518



Zastita Materijala 66 () (2025

# Corrosion Inhibition performance of 5-(3-hydroxyphenyl)-3-carboxyisoxazole for mild steel in acidic media: Experimental and theoretical insights

#### **ABSTRACT**

The present study investigates the corrosion inhibition efficiency of 5-(3-hydroxyphenyl)-3carboxyisoxazole (HPCI) for mild steel in 1.0 M hydrochloric acid solution using weight loss and electrochemical techniques. The weight loss method was employed to assess the effect of varying inhibitor concentrations (0.0-0.5 mM) at 303 K over different immersion times (1-48 hours). The influence of temperature (303-333 K) on the inhibition performance was also evaluated at these concentrations for a fixed 5-hour immersion period. The results indicate that inhibition efficiency increases with inhibitor concentration, achieving a maximum of 88.2% at 0.5 mM. Interestingly, a slight increase in efficiency with temperature was observed, suggesting physical adsorption as a predominant mechanism. Potentiodynamic polarization studies at 303 K for 5 hours immersion corroborated the weight loss findings and confirmed a mixed-type inhibition mechanism. Adsorption behavior of the inhibitor was found to obey the Langmuir adsorption isotherm model, supporting a monolayer adsorption on the metal surface. Density Functional Theory (DFT) calculations provided electronic descriptors such as the energy gap (ΔEgap) and the highest occupied molecular orbital energy (EHOMO), which confirmed the high electron-donating ability and strong adsorption potential of HPCI. The synergistic use of experimental and theoretical methods demonstrates the potential of 5-(3-hydroxyphenyl)-3-carboxyisoxazole as an efficient and environmentally friendly corrosion inhibitor for mild steel in acidic environments.

**Keywords:** Weight Loss method, potentiodynamic polarization, carboxyisoxazole, mild steel, corrosion inhibitor

# 1. INTRODUCTION

Mild steel (MS), a low-carbon alloy of iron, is one of the most extensively utilized engineering materials across a broad spectrum of industrial applications, including petrochemical processing, power generation, transportation infrastructure, and construction [1-3]. Its widespread use can be attributed to favorable properties such as high tensile strength, ductility, weldability, and, critically, its cost-effectiveness relative to other alloys. However, a major limitation in its service life and reliability is its inherent susceptibility to corrosion,

Corresponding author:

E-mail: dr.ahmed1975@gmail.com Paper received: 06.07.2025. Paper accepted: 05. 09.2025.

especially when exposed to aggressive media such as acidic solutions [4,5]. Hydrochloric acid (HCI), in particular, is frequently employed in processes like acid pickling, scale removal, descaling, and oil well acidizing, all of which expose mild steel to severe corrosion conditions [6,7]. The consequences of corrosion extend far beyond mere material degradation. According to global estimates by the National Association of Corrosion Engineers (NACE), corrosion-related losses account for approximately 3.5% of the global gross domestic product (GDP), equivalent to around US\$2.5 trillion annually [8,9]. These losses manifest in two broad categories: direct costs such as equipment replacement, maintenance, and shutdowns, and indirect costs including environmental damage, safety hazards, energy inefficiencies, and operational disruptions [10-12]. To mitigate the impact of corrosion, especially in acidic environments, the use of corrosion inhibitors (CIs) has emerged as one of the most efficient and economically viable strategies [13,14]. Corrosion inhibitors are chemical compounds that, when added in small concentrations to the corrosive medium, significantly reduce the rate of metal dissolution. Their mechanisms of action typically involve adsorption onto the metal surface, forming a protective barrier that blocks active corrosion sites and impedes the access of aggressive ions like Cl<sup>-</sup> and H<sup>+</sup> [15,16]. Among the various classes of corrosion inhibitors, organic compounds have received considerable attention due to their high inhibition efficiencies, versatile molecular architectures, and adaptability different corrosive environments [17]. These compounds usually contain heteroatoms such as nitrogen, oxygen, sulfur, and phosphorus, which facilitate their adsorption on metal surfaces via electron donation or back-donation mechanisms [18,19]. The presence of  $\pi$ -electrons in aromatic systems and conjugated double bonds further enhances their ability to interact with vacant dorbitals of metal atoms, contributing to stable and durable protective films [20]. Despite effectiveness, many conventional organic inhibitors are derived from synthetic sources that are often non-biodegradable, toxic, and environmentally hazardous. Consequently, the recent surge in environmental consciousness and stringent ecological regulations such as those from the OSPAR and REACH commissionshas propelled research toward developing sustainable, ecofriendly alternatives. These include corrosion inhibitors derived from plant extracts, amino acids, alkaloids, biopolymers, and pharmaceuticals [21,22].

For example, Umoren et al. (2015) examined the use of Phoenix dactylifera leaf extract as a green corrosion inhibitor for API 5L X60 steel in HCl. The extract, rich in flavonoids and phenolic compounds, demonstrated a synergistic effect with potassium iodide and formic acid, achieving inhibition efficiencies of up to 96.9% [23]. Similarly, Espinoza-Vázquez et al. (2019) reported the corrosion inhibition activity of carbohydrates such as glucose and lactose on mild steel, linking their performance to hydrogen bonding and electrostatic interactions [24].In parallel, theoretical approaches such as density functional theory (DFT) and molecular dynamics simulations have increasingly integrated into inhibitor design. These computational tools enable the prediction of adsorption energies, frontier molecular orbital (FMO) energies (EHOMO and ELUMO), and molecular electrostatic potential maps. For instance, Al-Amiery et al. (2022) investigated nonanedihydrazide using both experimental and DFT methods, confirming that the inhibitor followed the Langmuir isotherm and exhibited strong chemisorption behavior, supported by its electronic descriptors [25].

In the context of these advances, heterocyclic compounds such as isoxazoles have recently garnered attention for corrosion inhibition due to their electronic properties and structural features. Isoxazoles are five-membered aromatic rings containing one oxygen and one nitrogen atom, both of which act as electron-rich centers that can donate lone pairs to the metal surface. These compounds often contain substituent groups like hydroxyl (-OH), carboxylic acid (-COOH), and amide functionalities, which further enhance their adsorption capacity through hydrogen bonding and coordination interactions [26]. Specifically, 5-(3hydroxyphenyl)-3-carboxyisoxazole (HPCI) is an isoxazole derivative possessing both a hydroxyl and a carboxyl group, offering multiple active sites for interaction with the mild steel surface. The hydroxyl group may enhance electron density via resonance and inductive effects, while the carboxylic acid can deprotonate in aqueous media to form a carboxylate anion, further promoting adsorption via electrostatic and covalent interactions. Moreover, the  $\pi$ -system of the aromatic ring contributes to π-d orbital overlap with the metal surface, a phenomenon known to stabilize adsorbed layers. Despite these promising characteristics, literature documenting corrosion inhibition performance of HPCI is scant. To date, there have been few or no comprehensive studies evaluating its behavior **HCI** environments, particularly on mild steel. This represents a significant gap, considering the compound's structural potential for high inhibition efficiency. Despite extensive research into corrosion inhibition, there remains a need to explore novel, non-toxic, and efficient inhibitors that can perform effectively across varying operational conditions. Traditional inhibitors, while efficient, often pose environmental and health risks or suffer from reduced efficiency at elevated temperatures. Moreover, data on the efficacy of isoxazole particularly 5-(3-hydroxyphenyl)-3derivatives, carboxyisoxazole, in acidic media is scarce. The lack of comprehensive experimental and theoretical studies on this molecule limits its potential application as a viable inhibitor.This introduces 5-(3-hydroxyphenyl)-3-carboxyisoxazole (Figure 1) as a new corrosion inhibitor for mild steel in 1 M HCl solution. The novelty lies in:

 Employing a previously underexplored isoxazole derivative with dual functional groups.

- Comprehensive evaluation through weight loss, potentiodynamic polarization, and temperature studies.
- Correlating experimental inhibition efficiency with DFT-based electronic structure analysis to explain adsorption mechanisms.
- Investigating Langmuir adsorption isotherm behavior to establish monolayer formation.

To the best of our knowledge, this is the first systematic investigation combining these approaches for **HPCI** as а corrosion inhibitor. Therefore, the current study aims to address this gap by conducting a detailed experimental and theoretical investigation into the corrosion inhibition properties of HPCI for mild steel in 1 M HCl. This includes:

- Weight loss measurements at various concentrations (0.0 to 0.5 mM) and immersion times (1, 5, 10, 24, and 48 hours) at 303 K.
- Temperature variation studies (303–333 K) to evaluate thermodynamic parameters and the nature of the adsorption process.
- Potentiodynamic polarization measurements to classify the inhibitor as anodic, cathodic, or mixed-type.
- Adsorption isotherm modeling using the Langmuir model to determine surface coverage behavior.
- Density Functional Theory (DFT) calculations to elucidate electronic descriptors such as HOMO-LUMO energies and molecular electrostatic potential.

By integrating experimental techniques with quantum chemical calculations, this study not only establishes the effectiveness of HPCI as a corrosion inhibitor but also contributes to the broader scientific understanding of structure—activity relationships in organic inhibitors. The findings aim to pave the way for the development of new, environmentally sustainable corrosion prevention strategies for industrial systems operating in acidic environments. The primary goal of this research is to evaluate the corrosion inhibition performance of 5-(3-hydroxyphenyl)-3-carboxyisoxazole for mild steel in hydrochloric acid medium. The specific objectives include:

- Quantify inhibition efficiency using the weight loss method over various concentrations (0.0– 0.5 mM) and immersion times (1–48 h) at 303 K.
- 2. Examine the effect of temperature (303–333 K) on corrosion inhibition at fixed immersion time (5 h) and variable inhibitor concentrations.
- Analyze electrochemical behavior using potentiodynamic polarization to classify the inhibitor type and mechanism.

- 4. Investigate adsorption behavior through Langmuir isotherm analysis.
- Explore molecular interactions and electronic properties using Density Functional Theory (DFT) to establish structure–activity relationships.

Figure 1. Chemical structure of HPCI

#### MATERIALS AND METHODOLOGICAL FRAMEWORK

#### 2.1. Reagents and Inhibitor Verification

All chemicals applied in this investigation, including the targeted corrosion inhibitor 5-(3-hydroxyphenyl)-3-carboxyisoxazole (HPCI), were of analytical-grade purity and acquired from Sigma-Aldrich (Selangor, Malaysia). These substances were used without any subsequent refinement. The chemical integrity of HPCI was authenticated via thin-layer chromatography (TLC) using silica gel G-coated plates. This verification step ensured the absence of secondary species that could compromise the experimental reliability.

# 2.2. Substrate Preparation and Surface Conditioning

Flat coupons of mild steel served as the substrate in both gravimetric and electrochemical tests. The steel specimens, provided by Gamry Instruments Inc., possessed a defined exposed surface area of 4.5 cm². The elemental makeup (wt.%) of the mild steel was confirmed as follows: Fe – 99.21%, C – 0.21%, Si – 0.38%, P – 0.09%, S – 0.05%, Mn – 0.05%, and Al – 0.01%. Surface preparation adhered to the standardized protocol ASTM G1-03, which involved sequential polishing using emery papers of increasing grit (grades 400–1200), rinsing with deionized water, degreasing with acetone, and drying with warm air. This procedure was critical to ensure uniformity and reproducibility across all experimental runs [27,28].

# 2.3. Electrochemical Investigation Protocols

Electrochemical evaluations were conducted in an aerated 1.0 M HCl solution, prepared by diluting concentrated hydrochloric acid with distilled water. Different concentrations of HPCl (0.0–0.5 mM) were introduced to investigate its corrosion inhibition performance on mild steel. The experiments were carried out using a Gamry REF600 electrochemical workstation with a standard three-electrode configuration. Mild steel

coupons with a defined exposed surface area of 4.5 cm<sup>2</sup> were used as the working electrode. Each coupon was embedded in an inert, non-conductive resin holder to expose only one surface to the electrolyte, ensuring a well-defined active area. Electrical contact was established by soldering a copper wire to the unexposed rear side of the steel specimen, which was then insulated and connected to the electrochemical workstation. A saturated calomel electrode (SCE) served as the reference electrode, and a platinum mesh was used as the electrode. All measurements counter performed in static, naturally aerated solutions at ambient temperature. Prior to data acquisition, the working electrode was immersed in the test solution for 30 minutes to stabilize the open circuit potential (OCP) [29].

## 2.4. Polarization Curve Analysis

To quantify the corrosion inhibition effect, potentiodynamic polarization measurements were recorded. The working electrode potential was scanned within the ±200 mV window relative to the open-circuit potential (OCP) at a consistent rate of 0.5 mV·s<sup>-1</sup>. Prior to data acquisition, each electrode was immersed in the test solution for 30 minutes to reach electrochemical equilibrium. This conditioning period enabled stabilization of the double-layer capacitance and steady-state potential, thereby improving the reliability of the Tafel extrapolation results. The corrosion current density (Icorr) and potential (Ecorr) were extracted from the polarization plots to determine the inhibitor's mode of action [30].

### 2.5. Data Validation and Replication Strategy

Each test was independently repeated five times to confirm data repeatability. Mean values were computed and reported. Any results with a deviation exceeding 3% from the mean were excluded to maintain consistency and minimize experimental error.

#### 2.6. Static Immersion (Gravimetric) Analysis

Corrosion kinetics were also investigated using the classical weight loss method. Mild steel coupons (1 cm<sup>2</sup> exposed area) were immersed in 500 mL of HCl solution with and without inhibitor concentrations (0.1-0.5 mM). The test durations included 5, 10, 24, and 48 hours, and experiments were conducted at controlled temperatures (303 K, 313 K, 323 K, and 333 K), maintained using a thermostatically regulated water bath.Upon completion of each immersion period, samples were gently rinsed in ultrapure water and ethanol using an ultrasonic bath, followed by drying and reweighing [31]. Mass loss was recorded and used to compute corrosion rate (CR), inhibition efficiency (IE%), and surface coverage ( $\theta$ ) using the following formulations (1-3):

$$C_R = \frac{W}{at} \tag{1}$$

where W is the weight loss in grams, a is the exposed surface area of the steel sample in cm², and t is the immersion time in hours.

$$IE\% = \left[1 - \frac{c_{R(i)}}{c_{R(a)}}\right] \times 100$$
 (2)

Where: where  $C_{R(o)}$  is the corrosion rate without the inhibitor (control) and  $C_{R(i)}$  is the corrosion rate in the presence of BIHCC.

$$\theta = 1 - \frac{c_{R(l)}}{c_{R(o)}} \tag{3}$$

Figure 2 shows a simplified representation of the setup, in which a suspended steel sample is held in place within the acidic solution inside a glass beaker.

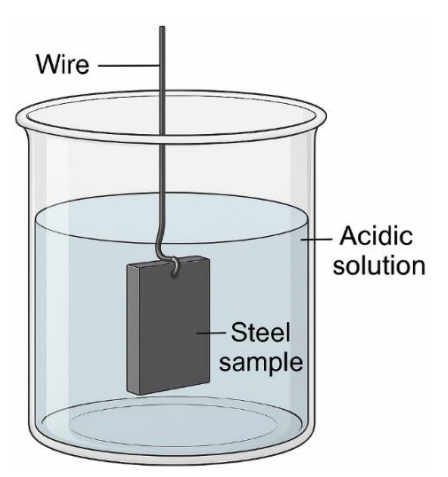


Figure 2. Experimental Setup for Weight Loss Corrosion Test

# 2.7. Quantum Chemical Modeling and Electronic Descriptor Evaluation

To supplement the empirical analysis, quantum chemical computations were conducted using GAMESS software to assess the reactivity profile of the HPCI molecule. Geometry optimization and molecular orbital analysis were performed at the DFT-B3LYP/6-31G(d) theoretical level [32,33]. The following electronic parameters were derived (4-8):

Ionization potential (I): 
$$I = -E_{HOMO}$$
 (4)

Electron affinity (A): 
$$A = -E_{LUMO}$$
 (5)

Electronegativity (
$$\chi$$
):  $\chi = \frac{I+A}{2}$  (6)

Chemical hardness (
$$\eta$$
):  $\eta = \frac{I-A}{2}$  (7)

Chemical softness (
$$\sigma$$
):  $\sigma = \eta^{-1}$  (8)

Additionally, the electron transfer capability  $(\Delta N)$  between the inhibitor and iron atoms of mild steel was evaluated via (9):

$$\Delta N = \frac{7 - \chi_{inh}}{2\eta_{inh}} \tag{9}$$

Where  $\chi_{\rm inh}$  and  $\eta_{\rm inh}$  refer to the electronegativity and hardness of the inhibitor, respectively. For these calculations, the reference values for iron (Fe) were taken as  $\chi_{\rm Fe}=7$  eV and  $\eta_{\rm Fe}=0$  eV.

#### 3. RESULTS AND DISCUSSION

#### 3.1. Potentiodynamic Polarization Measurements

Corrosion behavior of mild steel in 1 M HCl solution, both in the absence and presence of varying concentrations of 5-(3-hydroxyphenyl)-3-carboxyisoxazole (HPCl), was investigated using potentiodynamic polarization (PDP) techniques. These measurements provide valuable insight into the electrochemical kinetics of the anodic and cathodic reactions and help quantify the influence of the inhibitor on the corrosion rate and mechanism. Figure 3 displays the anodic and cathodic polarization curves for mild steel exposed to 1 M HCl with increasing concentrations of HPCl (0.0–0.5 mM). The progressive shift in curves demonstrates the inhibitor's effect on current density and corrosion potential.

From the Tafel curves shown in Figure 3, it is evident that the addition of HPCI results in a noticeable reduction in both anodic and cathodic current densities, confirming its classification as a mixed-type inhibitor. The suppression is more pronounced on the cathodic branches, indicating that HPCI more effectively hinders the hydrogen evolution reaction than the anodic metal dissolution

process. A slight shift in the corrosion potential  $(E_{corr})$  toward more positive values was also observed with increasing inhibitor concentration. While this anodic shift may suggest some influence on the anodic process, it is important to note that  $E_{corr}$  alone cannot confirm inhibition effectiveness.

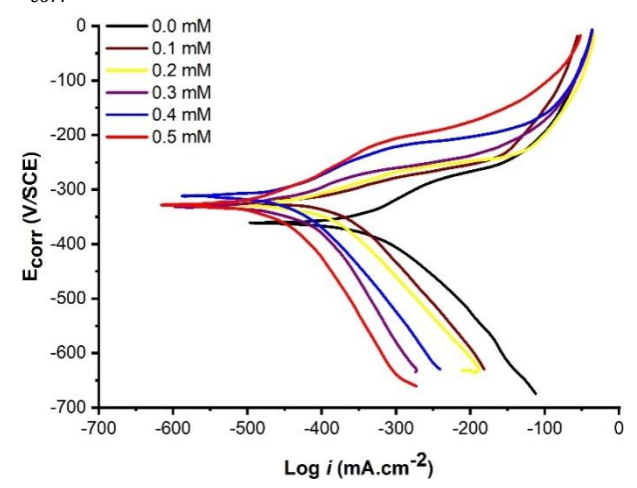


Figure 3. Tafel Polarization Curves of Mild Steel in 1 M HCl Containing Different Concentrations of HPCl

The classification of HPCI as a mixed-type inhibitor with a slight anodic predominance is supported by the combined trends in Tafel slopes and current densities. The maximum Ecorr shift from -0.460 V (blank) to -0.370 V at 0.5 mM indicates a notable modification of corrosion behavior, without altering the overall mechanism. Table 1 summarizes the electrochemical parameters derived from the Tafel plots, including corrosion potential ( $E_{corr}$ ), anodic ( $\beta_a$ ) and cathodic ( $\beta_c$ ) Tafel slopes, corrosion current density ( $I_{corr}$ ), and inhibition efficiency (IE%).

Table 1. Electrochemical Kinetic Parameters Derived from Polarization Curves for Mild Steel in 1 M HCl with Varying HPCI Concentrations

	T				
Conc. (mM)	$E_{corr}$ (V)	$\beta_a$ (mV/dec)	$-\beta_c$ (mV/dec)	$I_{corr}$ ( $\mu$ A/cm <sup>2</sup> )	IE (%)
0	-0.460	117	133	85.1	0.0
0.1	-0.440	109	121	61.7	27.5
0.2	-0.420	103	120	47.2	44.5
0.3	-0.410	99	109	39.6	53.5
0.4	-0.390	92	107	26.1	69.3
0.5	-0.370	87	96	10.1	88.1

The values in Table 1 illustrate a consistent decrease in corrosion current density as the concentration of HPCI increases. Without the inhibitor, Icorr is measured at 85.1  $\mu\text{A/cm}^2$ , but drops significantly to just 10.1  $\mu\text{A/cm}^2$  at 0.5 mM concentration an 88.1% inhibition efficiency. This decrease confirms the compound's strong surface-blocking capability, effectively reducing the

electrochemical reactivity of the mild steel surface. Furthermore, both the anodic ( $\beta a$ ) and cathodic ( $\beta c$ ) Tafel slopes decrease with rising HPCl concentration, suggesting that the inhibitor retards the kinetics of both electrode reactions [35]. This symmetrical shift in both slopes and the reduction in slope values point toward the adsorption of HPCl molecules at active sites, thereby altering the

reaction kinetics without changing the reaction mechanism. The high inhibition efficiency at relatively low concentrations demonstrates that HPCI forms a robust protective film, likely via chemisorption involving electron-donating groups such as -OH and -COOH, which enhance interaction with the mild steel surface. This behavior aligns with other studies where nitrogenand oxygen-containing heterocyclic compounds exhibit similar mixed-type inhibition profiles due to their polar functional groups and conjugated  $\pi$ systems. In summary, polarization measurements conclusively establish that 5-(3-hydroxyphenyl)-3carboxyisoxazole is an efficient and concentrationdependent corrosion inhibitor for mild steel in acidic environments. The compound not only reduces the corrosion current but also shifts the corrosion potential and modifies the reaction kinetics, supporting its classification as a mixed-type inhibitor with significant promise for industrial application [36].

Understanding the adsorption behavior of corrosion inhibitors is vital for elucidating the mechanisms by which they interact with metallic surfaces. Adsorption isotherms offer a quantitative framework to describe this interaction by relating the surface coverage of the inhibitor ( $\theta$ ) to its concentration in solution (C). In this study, several isotherm models were examined to interpret the adsorption behavior of HPCI on mild steel, including the Langmuir, Temkin, Freundlich, and Frumkin isotherms. The Langmuir isotherm assumes monolayer adsorption on a homogeneous

surface without interactions between adsorbed species. The Temkin isotherm considers interactions among adsorbed molecules and a linear decrease in adsorption heat with surface coverage. The Frumkin isotherm accounts for both adsorbateadsorbate and adsorbate-metal interactions, while the Freundlich isotherm is an model describina adsorption empirical heterogeneous surfaces. Among these models, the Langmuir isotherm provided the best linear fit to the experimental data, with a correlation coefficient (R2) of 0.813, compared to 0.725 for Temkin and 0.689 for Freundlich. The Frumkin model showed poor fitting behavior and was therefore not considered further (Figure 4).

Based on its superior fit and its suitability for monolayer adsorption of organic inhibitors, the Langmuir isotherm was selected to describe the adsorption behavior of HPCI on the mild steel surface [37]. To evaluate which model best fits our data, we examined the experimental from inhibition efficiencies (IE%) potentiodynamic measurements and calculated the corresponding surface coverage  $(\theta)$  values. The linearized form of the Langmuir isotherm is expressed as Equation (10):

$$\frac{C}{\theta} = \frac{1}{K_{ads}} + C \tag{10}$$

where:  $\mathcal{C}$  is the concentration of the inhibitor (mM),  $\theta$  is the surface coverage (calculated as IE% / 100), and  $K_{ads}$  is the equilibrium constant of adsorption.

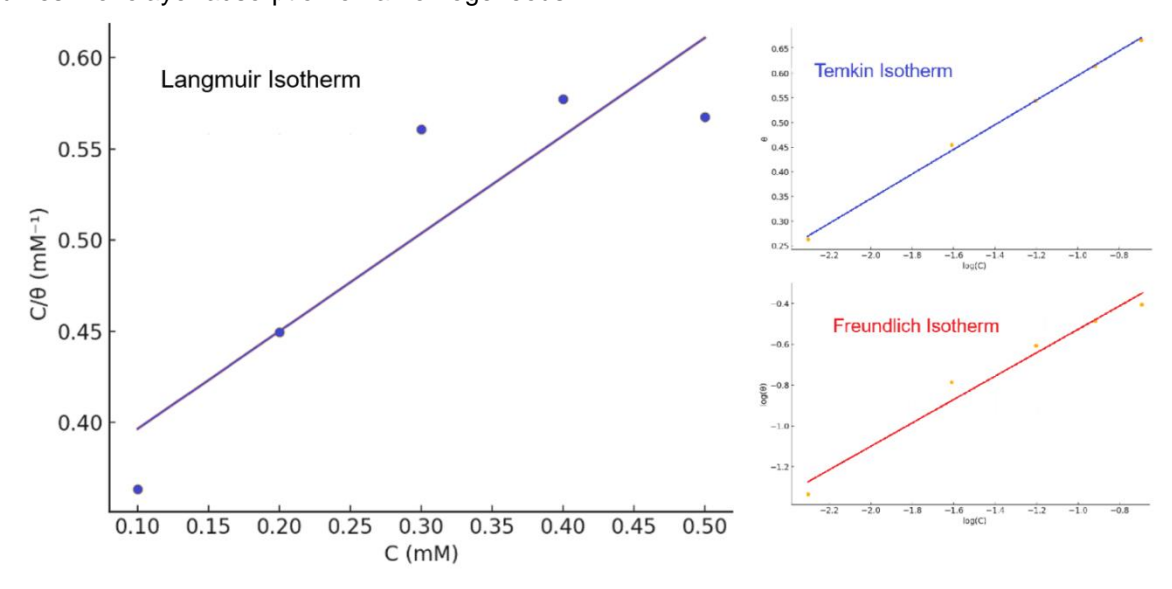


Figure 4. Langmuir, Temkin and FreundlichAdsorption Isotherms Plots for HPCI Adsorption on Mild Steel in 1 M HCI

By plotting  $C/\theta$  versus C, the data yielded a reasonably linear relationship with a coefficient of determination  $R^2$ =0.813, suggesting that the

Langmuir adsorption model adequately describes the adsorption behavior of HPCI on mild steel. Figure 4 represents the linear relationship between C/ $\theta$  and C supports Langmuir adsorption behavior, with surface coverage derived from polarization inhibition efficiencies. The moderate correlation coefficient (R<sup>2</sup> = 0.813) implies reasonably good conformity to the model [38]. The slope and intercept of the Langmuir plot also provide access to the adsorption equilibrium constant  $K_{ads}$ , which can be linked to the standard free energy of adsorption ( $\Delta G_{ads}^{0}$ ) using the equation (11):

$$\Delta G_{ads}^{\circ} = -RT ln(\mathbf{55.5} \times K_{ads}) \tag{11}$$

A higher  $K_{ads}$  value indicates adsorption affinity between the inhibitor and the mild steel surface, correlating with higher inhibition efficiency. While the deviation from perfect linearity might suggest minor lateral interactions or surface heterogeneity, the general fit confirms that HPCI primarily follows Langmuir-type monolayer adsorption. This analysis reinforces interpretation of potentiodynamic data indicating that HPCI forms a protective monolayer on the metal surface, significantly reducing the rate of anodic and cathodic reactions responsible for corrosion.

Using the slope of the Langmuir isotherm plot, the adsorption equilibrium constant  $K_{ads}$  was calculated to be approximately equal to 1.87 mM<sup>-1</sup>. Subsequently, the standard free energy of adsorption ( $\Delta G_{ads}^{\circ}$ ) was computed using the equation (11). Substituting the values R = 8.314J/mol·K, T=303 K, we obtain $\Delta G_{ads}^{\circ}$  equal to – 29.1 kJ/mol.The magnitude and sign of  $\Delta G_{ads}^{\circ}$  provide insight into the nature of the adsorption

process, if  $\Delta G_{ads}^{0}$  is around -20 kJ/mol or less, the adsorption is typically considered physisorption, involving electrostatic interaction between the inhibitor and the metal surface.If  $\Delta G_{
m ads}^{^0}$  is more negative than -40 kJ/mol, it generally indicates chemisorption, involving charge sharing or covalent bonding between the inhibitor and the metal atoms. Values between -20 and -40 kJ/mol suggest mixed adsorption, where both physical and chemical interactions coexist. Given that the computed value is -29.1 kJ/mol, the adsorption of 5-(3-hydroxyphenyl)-3-carboxyisoxazole on mild steel in HCl solution occurs via a mixed adsorption mechanism. This implies that, electrostatic attraction (physisorption) likely occurs between the protonated inhibitor molecules and negatively charged sites on the mild steel surface. Chemical interactions (chemisorption) may also be present due to lone pair electrons on heteroatoms (O, N) interacting with vacant d-orbitals of iron atoms, forming coordinate bonds. These combined effects contribute to the stability and effectiveness of the inhibitor film on the metal surface, as evidenced by the high inhibition efficiency and favorable thermodynamic profile.

#### 3.2. Open Circuit Potential Stabilization

Figure 5 illustrates the evolution of the open circuit potential (OCP) of mild steel in 1.0 M HCl over a 30-minute immersion period, both in the absence and presence of 0.5 mM HPCl. As shown, the OCP for the uninhibited (blank) solution initially shifts rapidly toward more negative values and gradually stabilizes around -0.500 V vs. SCE.

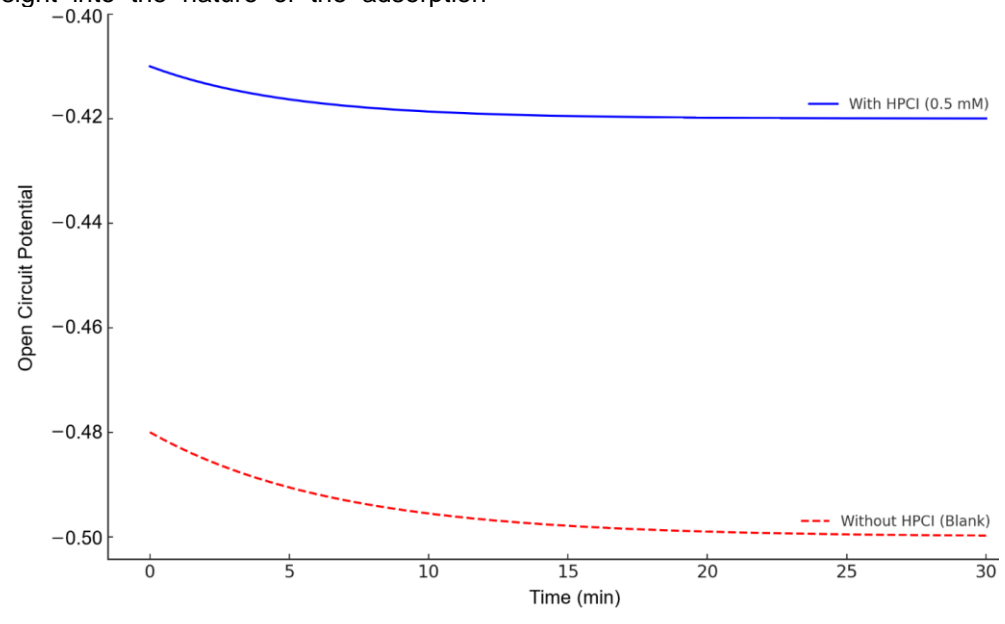


Figure 5. Variation of open circuit potential (OCP) of mild steel in 1.0 M HCl as a function of immersion time, with and without 0.5 mM HPCl. The HPCl-treated sample exhibits a more positive and earlier stabilization of potential, indicating the formation of a protective inhibitor film on the metal surface

This behavior reflects the active dissolution of mild steel in the acidic medium and the absence of any protective surface film. In contrast, the OCP of the HPCI-treated sample exhibits a distinctly different profile. The potential stabilizes more rapidly-within the first 20 minutes-and shifts to more positive values, ultimately stabilizing near -0.420 V vs. SCE. This anodic shift in potential suggests that the presence of HPCI impedes the anodic dissolution reaction of iron by forming a protective film at the metal-solution interface. The earlier and higher stabilization of the OCP confirms the rapid adsorption of HPCI molecules onto the mild steel surface and the establishment of an inhibitive layer before subsequent electrochemical measurements. These observations support the classification of HPCI as a mixed-type inhibitor with a slight anodic tendency and affirm the need for OCP stabilization prior to potentiodynamic polarization tests to ensure reliable interpretation.

#### 3.3. Static Immersion (Gravimetric) Analysis

complement the electrochemical investigation, gravimetric (weight loss) measurements were performed to assess the corrosion rate (CR) and inhibition efficiency (IE%) of 5-(3-hydroxyphenyl)-3-carboxyisoxazole (HPCI) on mild steel in 1 M HCl solution. This classical method provides a direct evaluation of metal mass loss over time and serves as a robust validation of corrosion inhibition behavior. The tests were conducted by immersing polished mild steel coupons into acidic solutions containing varying concentrations of the inhibitor (0.0-0.5 mM) at a constant temperature of 303 K for 5 hours. The mass loss of each specimen was recorded and used to calculate CR and IE according to standard equations. The results are illustrated graphically in Figure 6.

This dual-axis graph demonstrates the strong inverse relationship between HPCI concentration and CR (left Y-axis), along with a corresponding increase in IE (right Y-axis), indicating effective surface protection. The corrosion rate without any inhibitor was observed to be 3.10 mg·cm<sup>-2</sup>·h<sup>-1</sup>. indicating significant metal dissolution in the aggressive HCI medium. Upon introducing HPCI at just 0.1 mM, the CR dropped sharply to 1.11 mg·cm<sup>-2</sup>·h<sup>-1</sup>, corresponding to a 40.3% inhibition efficiency. As the inhibitor concentration increased, a further decline in corrosion rate was evident, culminating in a minimum CR of 0.32 mg·cm<sup>-2</sup>·h<sup>-1</sup> at 0.5 mM, with an associated IE of 88.2%. This progressive decrease in corrosion rate corresponding increase in inhibition efficiency confirms the concentration-dependent protection rendered by HPCI. The high efficiency at low dosages illustrates the compound's strong surface activity, which can be attributed to its functional groupshydroxyl (–OH) and carboxylic acid (–COOH)that promote adsorption through hydrogen bonding, electrostatic attraction, and potential chemisorption on the mild steel surface. The shape of the CR and IE curves (Figure 6) supports the monolayer adsorption assumption corroborated by the Langmuir isotherm model discussed previously [39].

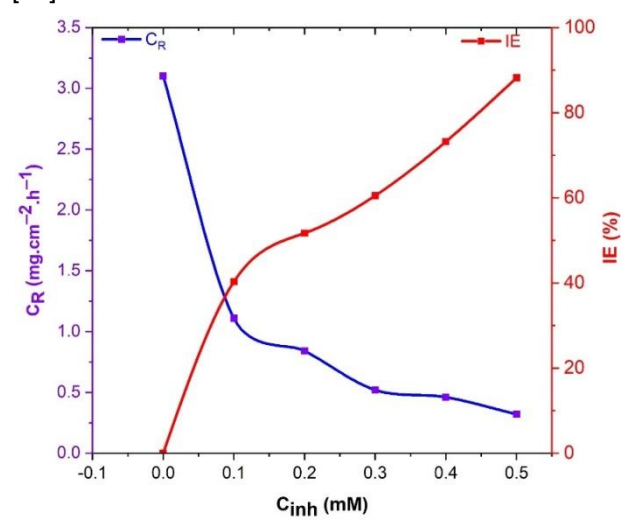


Figure 6. Effect of HPCI Concentration on Corrosion Rate (CR) and Inhibition Efficiency (IE%) of Mild Steel in 1 M HCI.

The non-linear but steady progression of IE with concentration suggests gradual surface coverage, eventually reaching saturation. Notably, the reduction in corrosion rate becomes less pronounced beyond 0.3 mM, hinting at an equilibrium state where available surface sites are nearly saturated with adsorbed inhibitor molecules. These findings are in close agreement with the polarization data, where similar trends in IE were observed, confirming the robustness of HPCI's inhibitive action across independent methodologies. Gravimetric analysis validates the potent corrosion inhibiting performance of HPCI in acidic environments. The results demonstrate a and efficient adsorption mechanism responsible for significant corrosion suppression of mild steel, with maximum protection achieved at 0.5 mM. This positions HPCI as a promising ecofriendly inhibitor candidate for industrial acid cleaning and pickling applications. To further understand the long-term stability and effectiveness of the inhibitor, the influence of immersion duration on corrosion rate and inhibition efficiency was assessed at various concentrations of HPCI over immersion periods of 1, 5, 10, 24, and 48 hours in 1 M HCl. The results are graphically depicted in Figure 7.

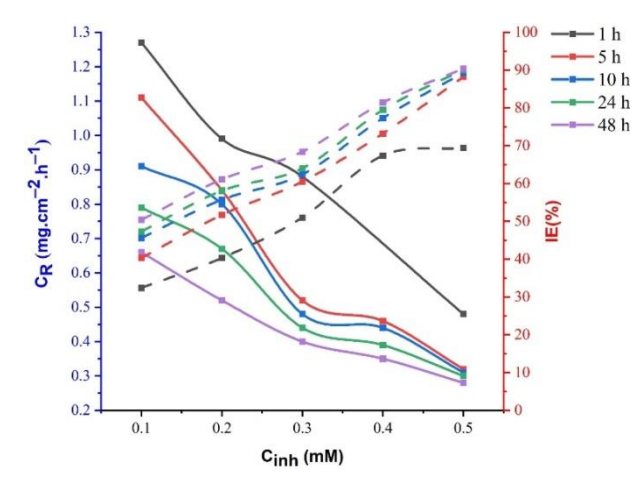


Figure 7. Effect of Immersion Time on Corrosion Rate (CR) and Inhibition Efficiency (IE%) at Various HPCI Concentrations

The figure illustrates the behavior of CR (solid lines, left axis) and IE% (dashed lines, right axis) as a function of immersion time (1-48 h) at different inhibitor concentrations (0.1-0.5 mM). For all inhibitor concentrations, the inhibition efficiency increased progressively with immersion time, demonstrating enhanced surface coverage and stabilization of the protective film formed by HPCI molecules. The trend is particularly significant within the first 10 hours, after which the rate of change becomes less pronounced, suggesting the onset of a saturation state. The protective effect of was consistently superior at higher concentrations across all immersion periods. At 0.5 mM, the IE% increased from 69.4% at 1 hour to 90.4% at 48 hours, highlighting excellent long-term stability and sustained inhibition behavior. This indicates that the inhibitor continues to effectively adhere to and protect the steel surface, resisting desorption or degradation even after prolonged exposure. For each concentration, a plateau in CR reduction and IE enhancement is observed beyond 24 hours. This may be attributed to the formation of a compact, adsorbed monolayer of HPCI on the metal surface, effectively impeding both anodic and cathodic reactions. Such stabilization is a desirable attribute for corrosion inhibitors in industrial applications involving extended contact times. At the lowest concentration (0.1 mM), the increase in inhibition efficiency was modestfrom 32.4% at 1 hour to 50.4% at 48 hoursimplying limited surface coverage and possibly less effective adsorption dynamics [41]. This reaffirms the importance of achieving an optimal concentration to ensure reliable protection. The immersion time study confirms that HPCI exhibits excellent timedependent inhibition behavior, particularly at higher concentrations. The progressive enhancement of IE% with immersion time suggests strong, stable adsorption of inhibitor molecules onto the mild steel surface. This adsorption leads to the formation of a durable barrier against acid attack, maintaining efficacy over extended periods. These findings highlight the potential of HPCI as a long-acting corrosion inhibitor suitable for industrial systems where materials are exposed to acidic environments over prolonged durations.

#### 3.4. Temperature Influence on Inhibition Behavior

Temperature plays a critical role in the corrosion process and the adsorption behavior of inhibitors. To evaluate the thermal stability and activation characteristics of 5-(3-hydroxyphenyl)-3-carboxyisoxazole (HPCI), static immersion tests were conducted at four different temperatures303 K, 313 K, 323 K, and 333 Kfor 5 hours immersion time at varying inhibitor concentrations (0.1–0.5 mM). The results are visualized in Figure 8.

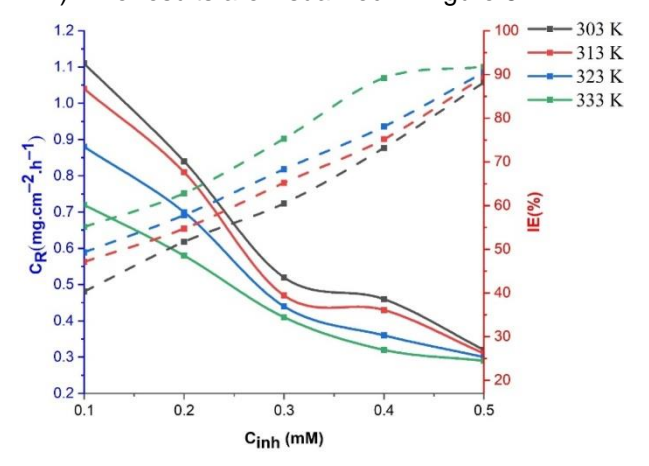


Figure 8. Influence of Temperature on Corrosion Rate (CR) and Inhibition Efficiency (IE%) at Various Concentrations of HPCI

Solid lines represent corrosion rate (left axis), and dashed lines show inhibition efficiency (right across increasing concentrations temperatures. The results reveal that the inhibition efficiency of HPCI remains high even as the temperature increases from 303 K to 333 K. For instance, at 0.5 mM concentration, IE increased slightly from 88.2% at 303 K to 91.8% at 333 K, suggesting a thermally stable protective layer on steel surface. Conventionally, corrosion inhibitors lose effectiveness elevated temperatures due to desorption or breakdown of adsorbed layers. However, the observed trend of increased inhibition efficiency with temperature for chemisorption-dominated indicates а mechanism, where the inhibitor forms strong chemical bonds with the metal surface. The rise in IE% with temperature implies that the interaction between the HPCI molecules and mild steel surface becomes more favorable thermodynamically at higher thermal energy levels, enhancing adsorption and compact film formation. temperature generally

corrosion, the presence of HPCI substantially reduces CR across all tested temperatures. For example, without the inhibitor, corrosion would increase exponentially with temperature; however, at 0.5 mM HPCI, CR remains nearly constant, decreasing slightly from 0.32 to 0.29 mg·cm<sup>-2</sup>·h<sup>-1</sup> from 303 K to 333 K.The thermal behavior of HPCI confirms its effectiveness as a robust, thermally stable inhibitor. The improved inhibition efficiency at elevated temperatures implies that HPCI primarily undergoes chemisorption on the mild steel surface. This characteristic is particularly advantageous for high-temperature applications such as acid cleaning in refineries, boilers, and chemical reactors where many inhibitors tend to fail

$$ln(C_R) = ln A - \frac{E_a}{TR}$$

Where:  $C_R$  is the corrosion rate, A is the preexponential factor,  $E_a$  is the activation energy (J/mol),R is the gas constant (8.314 J/mol·K), and T is the absolute temperature (K).

By plotting  $\ln(C_R)$  against 1/T, the slope of the linear fit gives  $-E_a/R$ , from which the activation energy can be calculated as in Figure 9.

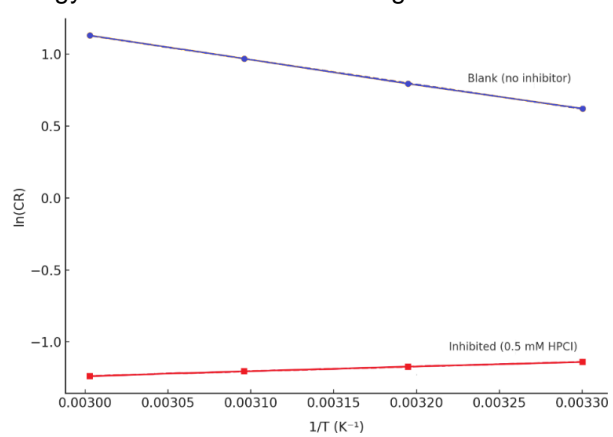


Figure 9. Arrhenius Plot for Corrosion of Mild Steel in 1 M HCl With and Without 0.5 mM HPCl

The calculate activation energy without inhibitor (Blank) was 14.23 kJ/mol and the activation energy with 0.5 mM HPCI was -2.75 kJ/mol. The positive value of 14.23 kJ/mol in the uninhibited solution confirms that the corrosion reaction is thermally

activated, increasing significantly with temperature. The surprisingly negative Ea value in the presence of 0.5 mM HPCI indicates a highly stable and strongly adsorbed inhibitor film, leading to a suppressed corrosion rate even at elevated temperatures. This behavior is associated with chemisorption, where the inhibitor forms strong chemical bonds with the metal surface, resulting in temperature-favored adsorption and enhanced stability of the protective layer. The stark contrast in activation energies between the blank and inhibited systems highlights a mechanistic shiftfrom surfacelimited metal dissolution in the uninhibited system to surface-protected and activation-suppressed corrosion in the presence of HPCI. The Arrhenius analysis reinforces earlier findings gravimetric electrochemical and evaluations, confirming that 5-(3-hydroxyphenyl)-3carboxyisoxazole acts through chemisorption, providing thermal resilience and highly efficient corrosion protection. Its low or negative activation energy further suggests a highly stable adsorption film that can perform under industrial thermal stresses.

#### 3.5. DFT-Based Molecular Analysis

To elucidate the electronic properties and adsorption behavior of 5-(3-hydroxyphenyl)-3carboxyisoxazole (HPCI) as a corrosion inhibitor, quantum chemical calculations were performed using Density Functional Theory (DFT) at the B3LYP/6-31G(d) level. The results provide insight into the molecule's reactivity, donor-acceptor characteristics, and ability to adsorb onto the mild steel surface through frontier molecular orbitals and associated descriptors. Figure 10(a) displays the energy-minimized structure of HPCI, showing its planarity and delocalized  $\pi$ -electron system. The presence of heteroatoms (O, N) is critical for surface interaction with mild steel [2,6,19]. The HOMO as in Figure 10(b) is primarily distributed over the isoxazole ring and adjacent aromatic system, indicating the active donor sites. These areas are capable of interacting with the d-orbitals of iron atoms via electron donation. The LUMO as in Figure 10(c) is localized near the carboxyl and hydroxyl groups, signifying potential sites for electron acceptance and back-donation from the metal surface.

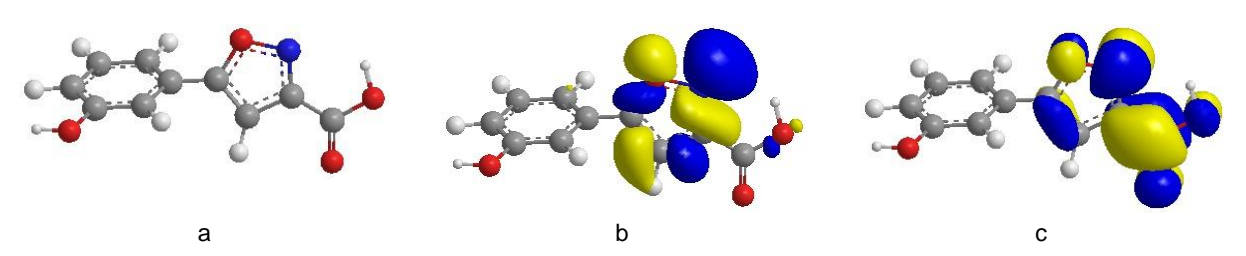


Figure 10. (a) Optimized Geometry of HPCI Molecule, (b) Highest Occupied Molecular Orbital (HOMO) Distribution of HPCI and (c) Lowest Unoccupied Molecular Orbital (LUMO) Distribution of HPCI

The energy gap between HOMO and LUMO is calculated as 8.121 eV, which, while relatively wide, is consistent with stable organic inhibitors (Table 2).

Table 2. Quantum Chemical Parameters Derived from HOMO and LUMO Energies

Parameter	Value	
Еномо (eV)	-11.312	
Eluмо (eV)	-3.191	
ΔE <sub>gap</sub> (eV)	8.121	
Ionization Potential (I, eV)	11.312	
Electron Affinity (A, eV)	3.191	
Electronegativity ( $\chi$ , eV)	7.2515	
Hardness (η, eV)	4.0605	
Softness (σ, eV <sup>-1</sup> )	0.246275089	
Chemical Potential (μ, eV)	-7.2515	
Electrophilicity Index (ω, eV)	6.475095709	
Electron Transfer (ΔN)	-0.030969092	

A moderate gap indicates a balance between reactivity and stability, suggesting HPCI can form stable interactions with the metal surface while resisting rapid degradation. A lower HOMO energy signifies the ability to donate electrons to vacant dorbitals of the metal, aiding in adsorption through coordination bonds. The HOMO localization around the isoxazole and aromatic systems makes these the prime regions for surface interaction [20,25]. This moderate LUMO value indicates the molecule can also accept electrons from filled metal orbitals, enabling back-donation. Such dual donor-acceptor capacity favors chemisorption, a trait already supported by the thermodynamic and kinetic data. The molecule has a strong tendency to attract electrons, which promotes favorable interactions with the metallic surface. The negative chemical potential value reflects its stability and high inhibition tendency. The moderate hardness indicates that the molecule resists charge deformation upon interaction, while the softness shows its polarizability an important attribute for effective surface coverage. This high value supports the capability of HPCI to accept electrons and engage in stabilizing interactions, aligning with its observed mixed-type inhibition behavior. The small negative  $\Delta N$  suggests that HPCI behaves slightly as an electron acceptor when interacting with iron (Fe), consistent with the observed LUMO orientation and partial back-donation behavior. The DFT-based descriptors validate that HPCI is an electronically active and surface-reactive molecule with ideal characteristics for corrosion inhibition [26,29]. The localization of its HOMO and LUMO orbitals around heteroatoms and  $\pi$ -systems supports its dual functionality as both electron donor and acceptor. The electronic structure, combined with its favorable adsorption energy, confirms that the molecule adsorbs on the mild steel surface via a predominantly chemisorptive mechanism, enhancing its stability and efficiency under acidic conditions.

#### 3.6. Proposed Corrosion Inhibition Mechanism

To consolidate experimental and theoretical findings, a proposed mechanism illustrating the interaction of 5-(3-hydroxyphenyl)-3-carboxyisoxazole (HPCI) with the mild steel surface in 1 M HCI is depicted in Figure 11.

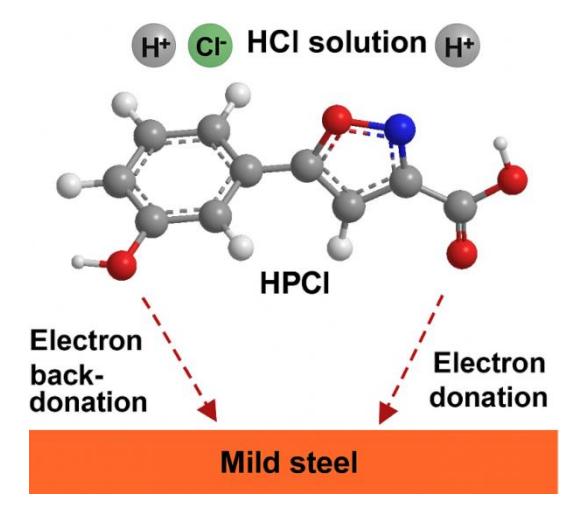


Figure 11. Suggested Mechanism of Corrosion Inhibition by HPCI on Mild Steel Surface

The schematic demonstrates adsorption of HPCI molecules onto the steel surface via lone-pair coordination,  $\pi$ -electron interaction, and hydrogen bonding. A protective film is formed, blocking active corrosion sites and impeding access to aggressive chloride and proton species. The inhibition mechanism is primarily governed by adsorption of HPCI molecules onto the metal surface, resulting in a barrier that hinders both anodic dissolution and evolution. cathodic hydrogen Under conditions, the nitrogen and oxygen atoms in HPCI may become partially protonated [40-42]. Despite protonation, lone pairs remain accessible, allowing the molecule to coordinate with vacant d-orbitals of Fe atoms. The carboxylic acid (-COOH) and hydroxyl (-OH) groups on the benzene ring act as electron donors through lone pairs on oxygen atoms. The isoxazole ring contains both nitrogen and oxygen heteroatoms, contributing additional electron density. The  $\pi$ -electron system of the heterocyclic aromatic and rinas enhances delocalization and stabilizes adsorption via π-d orbital overlap. These interactions suggest a chemisorption-dominant process, as supported by the negative  $\Delta G^{\circ}$  value (-29.1 kJ/mol), strong suppression of corrosion rates at elevated temperatures, localized HOMO density on active heteroatoms and ring systems (Figure 9), and DFTderived electrophilicity and softness values. The adsorbed HPCI molecules assemble into a thin, compact film on the steel surface. This laver physically blocks access of corrosive species (H+ and Cl<sup>-</sup>), disrupts the anodic dissolution of Fe<sup>2+</sup> ions, and suppresses hydrogen ion reduction by hindering electron flow to cathodic sites. While chemisorption plays the leading role, physisorption via electrostatic attraction between protonated HPCI and negatively charged sites may also contribute, especially during initial adsorption. This dual mechanism ensures quick adsorption followed by durable film formation. The proposed inhibition mechanism of HPCI on mild steel combines strong chemisorptive bonding via donor atoms and  $\pi$ systems, stable film formation observed in weight loss and electrochemical studies, and DFTvalidated electronic properties supporting effective metal-inhibitor interaction [43,44]. This multifaceted adsorption behavior explains the high inhibition efficiencies (>88%) and thermal stability observed during prolonged immersion and elevated temperatures. The inhibitor's structure makes it especially suitable for corrosion protection in aggressive acidic environments such as hydrochloric acid.

#### 4. CONCLUSION

In this study, the corrosion inhibition behavior of 5-(3-hydroxyphenyl)-3-carboxyisoxazole (HPCI) on mild steel in 1 M HCl solution was systematically investigated using a combination of weight loss techniques, potentiodynamic **DFT-based** polarization measurements, and chemical The quantum analysis. results unequivocally demonstrate that HPCI acts as a highly effective, stable, and environmentally compatible inhibitor with dual-mode activity. The key findings and conclusions drawn from this research include:

- Both gravimetric and electrochemical techniques showed that HPCI significantly reduced the corrosion rate of mild steel. The highest inhibition efficiency reached 88.2% at 0.5 mM concentration, with inhibition performance increasing with both concentration and immersion time.
- Potentiodynamic polarization studies revealed that HPCI inhibits both anodic and cathodic reactions, indicating a mixed-type inhibition mechanism with a slightly anodic predominance.

- Weight loss measurements across multiple immersion durations (1 to 48 h) and temperatures (303–333 K) confirmed the timedependent and thermally stable nature of the inhibitor. The inhibition efficiency remained above 90% at 48 h and 333 K, indicating durable adsorption and strong surface interaction.
- The inhibitor obeyed the Langmuir isotherm, suggesting monolayer adsorption on a homogeneous surface. The calculated free energy of adsorption (ΔG°<sub>ads</sub>) was -29.1 kJ/mol, confirming a spontaneous, mixed physical and chemical adsorption process.
- Arrhenius analysis revealed a significantly lower (even negative) activation energy in the presence of HPCI, supporting a chemisorptive mechanism that becomes more effective at elevated temperatures.
- DFT calculations identified key electronic descriptorsEHOMO = -11.312 eV, ELUMO = -3.191 eV, and ΔEgap = 8.121 eVthat confirmed strong donor–acceptor capacity. HOMO and LUMO distributions highlighted active adsorption sites on the isoxazole and phenol rings, aligning well with experimental inhibition performance.
- A schematic model was proposed showing HPCI adsorbing via lone-pair donation, π-d orbital interactions, and hydrogen bonding to form a stable protective film, effectively isolating the metal surface from aggressive species.

# Funding Statement

This research was funded by Al-Ayen Iraqi University (AUIQ) under the program 'Innovative Corrosion Inhibitors: A New Frontier in Materials Protection' (AUIQ-RFP2024-CI). The authors express their sincere gratitude for the financial support that made this study possible.

# Acknowledgment

The authors would like to express their heartfelt gratitude to Al-Ayen Iraqi University (AUIQ) for providing the financial support under the research project titled 'Innovative Corrosion Inhibitors: A New Frontier in Materials Protection' (Project Code: AUIQ-RFP2024-CI). Their assistance and resources were invaluable in the successful completion of this study.

#### Data availability

The datasets used and/or analysed during the current study available from the corresponding author on reasonable request.

#### Conflict of Interest

The authors declare no conflict of interest regarding the publication of this research article. All aspects of the study, including experimental design, data collection, analysis, and interpretation, were conducted with full academic and ethical integrity. The research was carried out independently, with no influence from funding agencies, organizations, or commercial entities that could result in a conflict of interest.

#### 5. REFERENCES

- [1] M. Errili, K. Tassaoui, A. Chraka, M. Damej, H. Rahal, N. Labjar, A. El Mahmoudi, K. Bougrin, A. Berisha, M. Benmessaoud (2024) Synthesis and investigation of novel sulfonamide–1,2,3–triazoles corrosion inhibitors for E24 steel in 1 M HCl solution: a combination of modeling and experimental approaches, Int. J. Corros. Scale Inhib., 13(3), 1607–1635. doi: 10.17675/2305-6894-2024-13-3-14
- [2] M.Y. El Sayed, A.M. Abdel-Gaber, H.T. Rahal(2019) Safranin – a potential corrosion inhibitor for mild steel in acidic media: a combined experimental and theoretical approach, J. Failure Anal. Prev., 19, 1174–1180. doi: 10.1007/s11668-019-00719-6
- [3] H.T. Rahal, A.M. Abdel-Gaber, G.O. Younes (2016) Inhibition of steel corrosion in nitric acid by sulfur containing compounds, Chem. Eng. Commun., 203(4), 435–445. doi: 10.1080/00986445.2015.1017636
- [4] H.T. Rahal, A.M. Abdel–Gaber, R. Awad (2016) Corrosion behavior of a superconductor with different SnO2 nanoparticles in simulated seawater solution, Chem. Eng. Commun., 204(3), 348–355. doi: 10.1080/00986445.2016.1271794
- [5] E.B. Caldona, M. Zhang, G. Liang, T.K. Hollis, C.E. Webster, D.W. Smith Jr and D.O. Wipf (2021) Corrosion inhibition of mild steel in acidic medium by simple azole-based aromatic compounds, J. Electroanal. Chem., 880, 114858. doi: 10.1016/j.jelechem.2020.114858
- [6] N. Benzbiria, A. Thoume, S. Echihi, M.E. Belghiti, A. Elmakssoudi, A. Zarrouk, M. Azzi and M. Zertoubi (2023) Coupling of experimental and theoretical studies to apprehend the action of benzodiazepine derivative as a corrosion inhibitor of carbon steel in 1 M HCl, J. Mol. Struct., 1281, 13513. doi: 10.1016/j.molstruc.2023.135139
- [7] R.D. Salim, N. Betti, M. Hanoon, A.A. Al-Amiery (2021) 2-(2,4-Dimethoxybenzylidene)-N-phenylhydrazinecarbothioamide as an efficient corrosion inhibitor for mild steel in acidic environment. Prog Color Colorant Coat, 15(1), 45–52. doi: 10.30509/pccc.2021.166775.1105
- [8] E.S. Sherif (2011) Corrosion and corrosion inhibition of aluminum in Arabian Gulf seawater and sodium chloride solutions by 3-amino-5-mercapto-1,2,4triazole, Int. J. Electrochem. Sci., 6(5), 1479–1492. doi: 10.1016/S1452-3981(23)15087-5

- [9] F.F. Sayyid, A.M. Mustafa, M.M. Hanoon, L.M. Saker, A.A. Alamiery (2022) Corrosion protection effectiveness and adsorption performance of schiff base-quinazoline on mild steel in HCl environment. CorrosSci Tech, 21(4), 77–88.
- [10] A. Altalhi (2023) Anticorrosion investigation of new diazene-based Schiff base derivatives as safe corrosion inhibitors for API X65 steel pipelines in acidic oilfield formation water: synthesis, experimental, and computational studies, ACS Omega, 8(34), 31271–31280. doi: 10.1021/acsomega.3c03592
- [11] A. Alobaidy, A. Kadhum, S. Al-Baghdadi, A. Al-Amiery, A. Kadhum, E. Yousif, A.B. Mohamad (2015) Eco-friendly corrosioninhibitor: experimental studies on the corrosion inhibition performance of creatinine for mild steel in HCl complemented with quantum chemical calculations. Int. J. Electrochem. Sci., 10(3), 3961–3972.
- [12] M. Ouakki, M. Galai and M. Cherkaoui (2022) Imidazole derivatives as efficient and potential class of corrosion inhibitors for metals and alloys in aqueous electrolytes: A review, J. Mol. Liq., 345, 117815. doi: 10.1016/j.molliq.2021.117815
- [13] X. Sun, Y. Qiang, B. Hou, H. Zhu and H. Tian (2022) Cabbage extract as an eco-friendly corrosion inhibitor for X70 steel in hydrochloric acid medium, J. Mol. Liq., 362, 119733. doi: 10.1016/j.molliq.2022.119733
- [14] M. Ghaderi, A.R. Saadatabadi, M. Mahdavian and S.A. Haddadi (2022) pH-Sensitive polydopamine-La (III) complex decorated on carbon nanofiber toward on-demand release functioning of epoxy anticorrosion coating, Langmuir, 38, 11707–11723. doi: 10.1021/acs.langmuir.2c01801
- [15] B.S. Mahdi, M.K. Abbass, M.K. Mohsin, W.K. Al-Azzawi, M.M. Hanoon, M.H.H. AlKaabi, L.M. Shaker, A.A. Al-Amiery, W.N.R.W. Isahak, A.A.H. Kadhum and M.S. Takriff (2022) Corrosion inhibition of mild steel in hydrochloric acid environment using terephthaldehyde based on Schiff base: Gravimetric, thermodynamic, and computational studies, Molecules, 27(15), 4857. doi: 10.3390/molecules27154857
- [16] A.J.M. Eltmimi, A. Alamiery, A.J. Allami, R.M. Yusop, A.H. Kadhum and T. Allam (2021) Inhibitive effects of a novel efficient Schiff base on mild steel in hydrochloric acid environment, Int. J. Corros. Scale Inhib., 10(2), 634–648. doi: 10.17675/2305-6894-2021-10-2-10
- [17] A. Alamiery, W.N.R.W. Isahak, H. Aljibori, H. Al-Asadi and A. Kadhum (2021) Effect of the structure, immersion time and temperature on the corrosion inhibition of 4-pyrrol-1-ylN-(2,5-dimethyl-pyrrol-1-yl)benzoylamine in 1.0 M HCl solution, Int. J. Corros. Scale Inhib., 10(2), 700–713. doi: 10.17675/2305-6894-2021-10-2-14
- [18] A.M. Resen, M.M. Hanoon, W.K. Alani, A. Kadhim, A.A. Mohammed, T.S. Gaaz, A.A.H. Kadhum, A.A. Al-Amiery and M.S. Takriff (2021) Exploration of 8piperazine-1- ylmethylumbelliferone for application as a corrosion inhibitor for mild steel in hydrochloric

- acid solution, Int. J. Corros. Scale Inhib., 10(1), 368–387. doi: 10.17675/2305-6894-2021-10-1-21
- [19] M.E. Ansar, K. Tassaoui, A. Chraka, R. Hsissou, M. Damej, H.T. Rahal, S. El Hajjaji and M. Benmessaoud (2024) Electrochemical, thermodynamic, and theoretical study of the corrosion inhibition properties of triglycidyloxy tripropylamine triazine on E24 steel in 1 M HCl, Int. J. Corros. Scale Inhib., 13(4), 2607–2637. doi: 10.17675/2305-6894-2024-13-4-38
- [20] F.F. Sayyid, S.I. Ibrahim, M.M. Hanoon, A.A.H. Kadhum and A.A. Al-amiery (2023) Gravimetric Measurements and Theoretical Calculations of 4-Aminoantipyrine Derivatives as Corrosion Inhibitors for Mild Steel in Hydrochloric Acid Solution: Comparative Studies, Corros. Sci. Technol., 22(2), 73–89. doi: 10.14773/CST.2023.22.2.73
- [21] M.H. Sliem, N.M. El Basiony, E.G. Zaki, M.A. Sharaf, A.M. Abdullah (2020) Corrosion Inhibition of Mild Steel in Sulfuric Acidby a Newly Synthesized Schiff Base: An Electrochemical, DFT, and Monte Carlo Simulation Study. Electroanalysis, 32, 3145– 3158, DOI: 10.1002/elan.202060461.
- [22] I. Obot, N. Obi-Egbedi, S. Umoren (2009) Antifungal drugs as corrosion inhibitors for aluminium in 0.1 M HCl. Corros. Sci, 51, 1868–1875, doi: 10.1016/j.corsci.2009.05.017.
- [23] M. Quraishi, F. Ansari, D. Jamal (2003) Thiourea derivatives as corrosion inhibitors for mild steel in formic acid. Mater. Chem. Phys, 77, 687–690, doi: 10.1016/S0254-0584(02)00130-X.
- [24] J. Fu, H. Zang, Y. Wang, S. Li, T. Chen, X. Liu (2012) Experimental and theoretical study on the inhibition performances of quinoxaline and its derivatives for the corrosion of mild steel in hydrochloric acid. Ind. Eng. Chem. Res, 51, 6377–6386, dol: 10.1021/ie202832e.
- [25] D.M. Jamil, A. Al-Okbi, M. Hanon, K.S. Rida, A. Alkaim, A. Al-Amiery, A. Kadhum, A.A.H. Kadhum (2018) Carbethoxythiazole corrosion inhibitor: as an experimentally model and DFT theory. J. Eng. Appl. Sci., 13(11), 3952–3959. doi: 10.3923/jeasci.2018.3952.3959
- [26] N.S. Abdelshafi, A.A. Farag, F.E.T. Heakal, A.S. Badran, K.M. Abdel-Azim, A.R. Manar El Sayed and M.A. Ibrahim (2024) In-depth experimental assessment of two new aminocoumarin derivatives as corrosion inhibitors for carbon steel in HCl media combined with AFM, SEM/EDX, contact angle, and DFT/MDS simulations, J. Mol. Struct., 1304, 137638. doi: 10.1016/j.molstruc.2024.137638
- [27] ASTM International, Standard Practice for Preparing, Cleaning, and Evaluating Corrosion Test, 2011, 1–9.
- [28] NACE International, Laboratory CorrosionTesting of Metals in Static Chemical Cleaning Solutions at Temperatures below 93°C (200°F), TM0193-2016-SG, 2000.
- [29] S.K. Saha, P. Ghosh, A. Hens, N.C. Murmu, P. Banerjee (2015) Density functional theory and molecular dynamics simulation study on corrosion inhibition performance of mild steel by mercapto-

- quinoline Schiff base corrosion inhibitor. PhysicaE, 66, 332–341, DOI: 10.1016/j.physe.2014.10.035.
- [30] A.S. Fouda, M.A. Ismail, A.M. Temraz, A.S. Abousalem (2019) Comprehensive investigations on the action of cationic terthiophene and bithiophene as corrosion inhibitors: experimental and theoretical studies. New J. Chem, 43, 768–789, DOI: 10.1039/C8NJ04330B.
- [31] A.M. Mustafa, F.F. Sayyid, N. Betti, M.M. Hanoon, A. Al-Amiery, A.A.H. Kadhum, M.S. Takriff (2021) Inhibition evaluation of 5-(4-(1H-pyrrol-1-yl)phenyl)-2-mercapto-1,3,4-oxadiazole for the corrosion of mild steel in an acid environment: thermodynamic and DFT aspects. Tribologia, 38(4), 39-47. https://doi.org/10.30678/FJT.105330
- [32] M.J. Frisch, G.W. Trucks, H.B. Schlegel, G.E. Scuseria, M.A. Robb, J.R. Cheeseman, J.A. Montgomery, T. Vreven, K.N. Kudin, J.C. Burant, J.M. Millam, S.S. Iyengar, J. Tomasi, V. Barone, B. Mennucci, M. Cossi, G. Scalmani, N. Rega, N. Petersson, H. Nakatsuji, H. Hada, M. Ehara, R. Toyota, R. Fukuda, J. Hasegawa, M. Ishida, T. Nakajima, Y. Honda, O. Kitao, H. Nakai, M. Klene, X. Li, J.E. Knox, H.P. Hratchian, J.B. Cross, V. Bakken, C. Adamo, J. Jaramillo, R. Gomperts, R.E. Stratmann, O. Yazyev, A.J. Austin, R. Cammi, C. Pomelli, J.W. Ochterski, J.W. Ayala, P.Y. Morokuma, G.A. Voth, P. Salvador, J.J. Dannenberg, V.G. Zakrzewski, S. Dapprich, A.D. Daniels, M.C. Strain, O. Farkas, D.K. Malick, A.D. Rabuck, K. Raghavachari, J.B. Foresman, J.V. Ortiz, Q. Cui, A.G. Baboul, S. Clifford, J. Cioslowski, B.B. Stefanov, G. Liu, A. Liashenko, P. Piskorz, I. Komaromi, R.L. Martin, R.L. Fox, T. Keith, M.A. Al-Laham, C.Y. Peng, Nanayakkara, M. Challacombe, P.M.W. Gill, B. Johnson, W. Chen, M.W. Wong, C. Gonzalez, J.A. Pople (2004) Gaussian 03, Revision B. 05, Gaussian, Inc., Wallingford, CT.
- [33] T. Koopmans (1934) Ordering of wave functions and eigenenergies to the individual electrons of an atom. Physica, 1(4), 104–113 (In German).
- [34] P.T. Scaria, P. Shetty, P. Preethi and S. Kagatikar (2022) 2-Aminobenzothiazole as an efficient corrosion inhibitor of AA6061-T6 in 0.5 M HCI medium: electrochemical, surface morphological, and theoretical study, J. Appl. Electrochem., 52( 11), 1–15, doi: 10.1007/s10800-022-01742-6
- [35] R. Yıldız (2015) An electrochemical and theoretical evaluation of 4,6-diamino-2- pyrimidinethiol as a corrosion inhibitor for mild steel in HCl solutions, Corros. Sci., 90, 544–553. doi: 10.1016/j.corsci.2014.10.047
- [36] X. Li, S. Deng and X. Xie (2014) Experimental and theoretical study on corrosion inhibition of oxime compounds for aluminium in HCl solution, Corros. Sci., 81, 162–175. doi: 10.1016/j.corsci.2013.12.021
- [37] O.J. Redlich and D.L. Peterson (1959) A Useful Adsorption Isotherm, J. Phys. Chem., 63(6) 1024. doi: 10.1021/j150576a611
- [38] K.Y. Foo and B.H. Hameed (2010) Insights into the modeling of adsorption isotherm systems, Chem. Eng. J., 156(1) 2–10. doi: 10.1016/j.cej.2009.09.013

- [39] S. Martinez (2003) Inhibitory Mechanism of Mimosa Tannin Using Molecular Modeling and Substitutional Adsorption Isotherms, Mater. Chem. Phys., 77, 97– 102. doi: 10.1016/S0254-0584(01)00569-7
- [40] M. Kilo, H.T. Rahal, M.H. El-Dakdouki and A.M. Abdel-Gaber (2021) Study of the corrosion and inhibition mechanism for carbon steel and zinc alloys by an eco-friendly inhibitor in acidic solution, Chem. Eng. Commun., 208(12) 1676–1685. doi: 10.1080/00986445.2020.1811239
- [41] E. Oguzie, Y. Li, S. Wang and F. Wang (2011) Understanding corrosion inhibition mechanisms – Experimental and theoretical approach, RSC Adv., 1(5), 866–873. doi: 10.1039/C1RA00148E
- [42] L. Guo, W. Dong and S. Zhang (2014) Theoretical challenges in understanding the inhibition

- mechanism of copper corrosion in acid media in the presence of three triazole derivatives, RSC Adv., 4, 41956–41967. doi: 10.1039/C4RA04931D
- [43] L. Guo, C. Qi, X. Zheng, R. Zhang, X. Shen and S. Kaya (2017) Toward understanding the adsorption mechanism of large size organic corrosion inhibitors on an Fe(110) surface using the DFTB method, RSC Adv., 7, 29042–29050. doi: 10.1039/C7RA04120A
- [44] A. Kahyarian, A. Schumaker, B. Brown and S. Nesic (2017) Acidic corrosion of mild steel in the presence of acetic acid: Mechanism and prediction, Electrochim. Acta, 258, 639–652. doi: 10.1016/j.electacta.2017.11.109

### **IZVOD**

# INHIBICIJA KOROZIJE 5-(3-HIDROKSIFENIL)-3-KARBOKSIIZOKSAZOLA ZA MEKI ČELIK U KISELIM SREDINAMA: EKSPERIMENTALNI I TEORIJSKI UVIDI

U ovoj studiji se istražuje efikasnost inhibicije korozije 5-(3-hidroksifenil)-3-karboksiizoksazola (HPCI) za meki čelik u 1,0 M rastvoru hlorovodonične kiseline korišćenjem tehnika gubitka težine i elektrohemijskih tehnika. Metoda gubitka težine je korišćena za procenu efekta različitih koncentracija inhibitora (0,0-0,5 mM) na 303 K tokom različitih vremena potapanja (1-48 sati). Uticaj temperature (303-333 K) na inhibicione performanse je takođe procenjen pri ovim koncentracijama tokom fiksnog perioda potapanja od 5 sati. Rezultati pokazuju da se efikasnost inhibicije povećava sa koncentracijom inhibitora, dostižući maksimum od 88,2% pri 0,5 mM. Zanimljivo je da je primećen blagi porast efikasnosti sa temperaturom, što ukazuje na fizičku adsorpciju kao dominantan mehanizam. Studije potenciodinamičke polarizacije na 303 K tokom 5 sati potapanja potvrdile su nalaze gubitka težine i potvrdile mehanizam inhibicije mešovitog tipa. Utvrđeno je da se ponašanje inhibitora pri adsorpciji podudara sa Lengmirovim modelom izoterme adsorpcije, što podržava monoslojnu adsorpciju na površini metala. Proračuni Teorije funkcionala gustine (DFT) dali su elektronske deskriptore kao što su energetski jaz (DEgap) i najviša zauzeta molekularna orbitalna energija (EHOMO), što je potvrdilo visoku sposobnost donorstva elektrona i snažan adsorpcioni potencijal HPCI. Sinergistička upotreba eksperimentalnih i teorijskih metoda pokazuje potencijal 5-(3-hidroksifenil)-3-karboksiizoksazola kao efikasnog i ekološki prihvatljivog inhibitora korozije za meki čelik u kiselim sredinama.

**Ključne reči:** Metoda gubitka težine, potenciodinamička polarizacija, karboksiizoksazol, meki čelik, inhibitor korozije

Naučni rad

Rad primljen: 06.07.2025. Rad prihvaćen: 05.09.2025.

Ayad Abbood Abdulhasan FirasF.Sayyid M.Mustafa Ahmed A. Alamiery, Abdul Amir H. Kadhum https://orcid.org/0009-0008-3272-5109 https://orcid.org/0000-0002-6817-335XAli https://orcid.org/0000-0002-5226-0926 https://orcid.org/0000-0003-1033-4904 https://orcid.org/0000-0003-4074-9123

<sup>© 2025</sup> Authors. Published by Engineering Society for Corrosion. This article is an open access article distributed under the terms and conditions of the Creative Commons Attribution 4.0 International license (https://creativecommons.org/licenses/by/4.0/)